Naval Research Laboratory

Washington, DC 20375-5320

NRL/MR/6700--96-7840

Linear Theory of a Large Volume, High Power Gyro Traveling Wave Amplifier

WALLACE MANHEIMER

Plasma Physics Division
Information Technology Division

May 1, 1996

19960514 081

Approved for public release; distribution unlimited.

DTIC QUALITY INSPECTED 1

REPORT DOCUMENTATION PAGE

Form Approved
OMB No. 0704-0188

Public reporting burden for this collection of information is estimated to average 1 hour per response, including the time for reviewing instructions, searching existing data sources, gathering and maintaining the data needed, and completing and reviewing the collection of information. Send comments regarding this burden estimate or any other aspect of this collection of information, including suggestions for reducing this burden, to Washington Headquarters Services, Directorate for Information Operations and Reports, 1215 Jefferson Davis Highway, Suite 1204, Arlington, VA 22202-4302, and to the Office of Management and Budget. Paperwork Reduction Project (0704-0188), Washington, DC 20503.

1. AGENCY USE ONLY *(Leave Blank)*	2. REPORT DATE	3. REPORT TYPE AND DATES COVERED
	May 1, 1996	Interim

4. TITLE AND SUBTITLE

Linear Theory of a Large Volume, High Power Gyro Traveling Wave Amplifier

5. FUNDING NUMBERS

PE - 0602234N

6. AUTHOR(S)

Wallace M. Manheimer

7. PERFORMING ORGANIZATION NAME(S) AND ADDRESS(ES)

Naval Research Laboratory
Washington, DC 20375-5320

8. PERFORMING ORGANIZATION REPORT NUMBER

NRL/MR/6700--96-7840

9. SPONSORING/MONITORING AGENCY NAME(S) AND ADDRESS(ES)

Office of Naval Research
800 North Quincy Street
Arlington, VA 22217-5660

10. SPONSORING/MONITORING AGENCY REPORT NUMBER

11. SUPPLEMENTARY NOTES

12a. DISTRIBUTION/AVAILABILITY STATEMENT

Approved for public release; distribution unlimited.

12b. DISTRIBUTION CODE

13. ABSTRACT *(Maximum 200 words)*

At a given cavity mode, as the wavelength decreases, the power capability of a microwave tube amplifier also decreases because the sizes get smaller. High power gyrotron oscillators have been developed by going to very high order cavity modes. So far this has not been accomplished for amplifiers, and it is not clear whether one could in fact do this. This paper examines another approach to the problem, namely the use of a quasi-optical beam (Gaussian mode) waveguide gyrotron amplifier. A closely related concept is the use of corrugated waveguide. This paper works out the linear theory of the device. Our conclusion is that it should work for an amplifier at 94 GHz having peak power of hundreds of kilowatts and average power of tens of kilowatts.

14. SUBJECT TERMS

Quasi-Optical gyro amplifier
Gyro amplifier

15. NUMBER OF PAGES

31

16. PRICE CODE

17. SECURITY CLASSIFICATION OF REPORT	18. SECURITY CLASSIFICATION OF THIS PAGE	19. SECURITY CLASSIFICATION OF ABSTRACT	20. LIMITATION OF ABSTRACT
UNCLASSIFIED	UNCLASSIFIED	UNCLASSIFIED	UL

NSN 7540-01-280-5500

Standard Form 298 (Rev. 2-89)
Prescribed by ANSI Std 239-18
298-102

CONTENTS

1. Introduction 1

2. General Formation 5

3. Calculation of $\int P_1^* J_x$ 7

4. Instability Condition 12

5. Results and Discussion 14

Appendix: The Effect of Prebunching in the Linear Regime 18

References 20

Acknowledgements 22

LINEAR THEORY OF A LARGE VOLUME, HIGH POWER GYRO TRAVELING WAVE AMPLIFIER

1. Introduction

This paper discusses a new concept for a high power millimeter wave gyro amplifier. While it is potentially viable at any short wavelength, we particularly focus on 94 GHz, the clearest part of the atmospheric propagation window. Also we envision this concept as a rf source for a large, fixed facility such as the Haystack or Kwajalein Radar facility, each managed by Lincoln Laboratory. Both of these antennas are qualified for radiation at 94 GHz. The former could accept an rf source of the size we propose now. For the latter, some reengineering of the facility would have to be done.[1]

The basic source concept is shown in Fig.(1), and a modified version is shown in Fig.(2). Instead of a waveguide configuration, it utilizes Gaussian radiation beams directly. This is advantageous, particularly for the projects of interest to Lincoln Laboratory. They have developed a number of high power components for Gaussian beams which we will discuss shortly. While their inventions were intended for the beam transmission system, there is no reason they cannot be used directly in the amplifier itself.

As an alternative configuration one could also use a corrugated waveguide with mitre bend reflectors, shown in Fig. 3, or with U bends (not shown). This corrugated waveguide supports TEM modes having very low loss. The waveguide is shown with large gaps near the point of electron beam traversal. These large gaps are to eliminate cutoff modes of the waveguides at these locations, as these would be the most likely competing modes. Since the transverse mode structure in both the quasi-optical and corrugated waveguide configurations are each nearly Gaussian in structure, we analyze here the beam interaction with Gaussian modes.

The configuration in Fig.(1) has a radiation field bouncing between mirrors in a serpentine path going from right to left. A gyrotron electron beam (i.e. one with transverse energy) propagates through the center of the radiation spot on the vertical radiation legs in the figure. As it propagates, it gives energy to the fields in a modified version of the gyro traveling wave amplifier (TWA) interaction. This configuration was motivated by earlier work at NRL on a gyroamplifier in a folded waveguide system[2], shown schematically in Fig. (4). However in the waveguide system, even at 35 GHz, the waveguide is quite small in the transverse direction,

Manuscript approved March 18, 1996.

thereby limiting the power capability. Our configuration is also motivated by other work at NRL on the quasi-optical gyrotron[3,4], shown schematically in Fig.(5). Here the gyrotron cavity was a Fabry Periot resonator oriented perpendicular to the magnetic field. As the beam traverses the resonator, it gives energy to the fields via the conventional gyrotron interaction. Recently it was also pointed out that the MIT group has also analyzed a configuration similar to this.[5] Their analysis relied mostly on particle simulation. This work here complements that by offering analytic theory.

Experience in running this device over about 5 years has shown that it operates basically as a gyrotron, but at somewhat less efficiency[6,7]. This can be partially compensated by the relative ease of incorporating a depressed collector, due to the fact that the beam and radiation propagate orthogonally. The best results of the experiments so far show an efficiency of 20%, which has been increased to 30% with a very simple single stage depressed collector. The quasi-optical gyrotron has a high axial mode density, but only a single transverse mode has ever been observed. Recent work has shown a number of ways in which the device can operate efficiently in a preselected axial mode. One of the ways has been to use a prebunching cavity. This prebuncing cavity is also shown in Fig.(5). It was powered by an extended interaction oscillator (EIO) at 85 GHz. The prebunched beam either excited the main cavity as an amplifier for the case where the main cavity was stable, or else controlled it as a phase locked oscillator for the case where the main cavity was unstable, but not very far above threshold. This amplifier should be capable of high average power, since the size of all components are large.

It is important that amplifier operation has been demonstrated on the quasi-optical gyroklystron. Nevertheless the device is not suitable as an amplifier if reasonable bandwidth is desired. Since the cavity mode has very high Q the bandwidth was only a few MHz. However with the experience obtained in the quasi-optical gyrotron and gyroklystron, it is natural to propose quasi-optical gyrotron traveling wave amplifier for the case where reasonable bandwidth is desired.

The configurations shown in Figs. (1 and 2) appear to have several advantages over waveguide configurations. First of all, the mode density is low. Assuming that the region outside of the ray

path uses millimeter wave absorbers, the only allowed modes are the modes of interest themselves. We envision a forward wave interaction. Since this mode cannot be absolutely unstable, it cannot oscillate without a source to drive it. However the backwards mode can also propagate, and this might be absolutely unstable depending on the current and length of the system. Typically in such a case, one either designs the amplifier short enough to be below oscillation threshold, or else uses severs in the circuit. As we will see, another possibility in this configuration is the use of a high power Gaussian mode circulator, developed at Lincoln Laboratory.

A particular advantage of the configuration proposed is that there is no zero group velocity mode. In traveling wave amplifiers, it is almost always the cutoff mode that interferes with operation by breaking into spontaneous oscillation. In the corrugated waveguide configuration of Fig. (3), the portion of the guide in which a cutoff mode is most likely to be excited, has been removed. Furthermore, we will also see that for electron beam energies of interest, if the amplifier is stabilized at a cyclotron harmonic n, it is also stabilized for all other harmonics p as long as p>n. Finally, it is clear that in the quasi-optical gyro TWA, the sizes of all components are relatively large, meaning that the power handling capability is also. The development of such an amplifier with peak power of 100 kW and average power in excess of 10 kW appears to be achievable.

Let us now continue by discusing two inventions developed at Lincoln Laboratory[8,9] which could render simpler the development of the quasi-optical gyro TWA. The first is the clam shell reflector shown in Fig. (6). When a Gaussian beam reflects obliquely from a spherical mirror, there is some depolarization. By utilizing the double mirror system shown (the clam shell), the depolarization in the first mirror is reversed in the second, so the polarization is preserved. Each mirror in Fig. (1) might be a clamshell; alternately, if the clam shell mirrors can be separated, the two adjacent mirrors in each horizontal leg can be a clam half of a clam shell.

The second is the quasi-optical millimeter wave circulator shown in Fig. (7). It utilizes a ferrite to rotate the polarization of the radiation 45°. Typically a permanent magnet is used with a field just large enough to drive the ferrite into saturation. Here the losses in the ferrite are minimized. However it is also possible to use the main field of the gyro TWA, although this is a much larger field than

would ordinarily be used. These ferrites are typically very lossy at the cyclotron resonance, but not so lossy at other frequencies[10]. Particularly, if the radiation is at twice the cyclotron frequency, the losses in the ferrite are not that large. The circulator can then be used in the circuit, for instance along the horizontal legs of Fig. (1) to prevent the backward wave from propagating through the system. It can be used as an alternative to the sever, but with the advantage that one does not have to worry about dumping the partially amplified radiation somewhere in the tube (ie at the sever). Furthermore, if the gyro TWA operates at the harmonic, the circulator can not only decouple the backward wave, but also provide strong dissipation at the fundamental.

This paper analyzes the linear theory of the quasi-optical gyro TWA. In Section 2, the general formalism is introduced. Section 3 calculates what is essentially E• J for the configuration. This quantity is needed to calculate the linear dispersion relation. Section 4 calculates the instability condition. Basically this calculates the maximum length, either for the entire system or between severs or circulators. Section 5 gives a few examples and results. In a sense the quasi-optical gyro TWA is the complement of the waveguide system. Where the latter is fighting large sizes, the former is fighting large size. Typically we find system lengths of half a meter to a meter and magnet bores of 4 to 6 inches. The appendix shows that in the linear regime, the klystron effect, that is the bunching of the beam in one vertical leg, followed the extraction in the next, is negligibly small.

2. General Formulation

In Fig. (1), let the plane of the paper be the yz plane with the constant magnetic field being in the z direction. The natural polarization for the electromagnetic wave in a gyrotron configuration is then the x direction. Maxwell's equations for this component reduce to

$$\nabla x \nabla x E_x \mathbf{i}_x + (1/c)^2 \mathbf{i}_x \partial^2 E_x/\partial t^2 = -\mathbf{i}_x (4\pi/c^2) \partial J_x/\partial t \qquad (1)$$

The configuration as shown in Figs.(1) is periodic with periodicity length L in the z direction, and confined radially to be within the outer conductor. Therefore,by Floquet's theorem, all quantities (E,J etc) can be expressed as a periodic function of z times an exponential exp ikz. Further, we imagine that the ray bounces around in the periodicity cell along some ray path, the distance along which is denoted by l. If we assume the wave propagates strictly in one direction, say to the right in Fig. (1), neglect diffraction, and the coupling to the backwards wave, Eq. (1) may be reduced to a single first order scalar equation

$$\partial E_x/\partial t + c\partial E_x/\partial l = -2\pi J_x \qquad (2)$$

and

$$E_x = P(y,z) \exp i(kz - \omega t) \qquad (3)$$

where P(y,z) is periodic in z with periodicity length L. Now say that the actual ray path the radiation traverses within a periodicity cell has length Λ. Let $r_\perp$ be the spatial variable describing the radiation profile perpendicular to l. Then let us take as an approximation for P, the function

$$P = R(r_\perp) \exp i[kLl/\Lambda - kz] \qquad (4)$$

Note that as the wave propagates a distance Λ, z advances a distance L so that P is periodic in z with periodicity length L. For the case we will consider here, R is a Gaussian with spot size r_o,

$$R(r_\perp) = \exp -(r/r_o)^2 \qquad (5)$$

Let us now stipulate that the electric field E_x can be decomposed into a summation of orthogonal functions

$$E_x = \Sigma_i \alpha_i P_i \tag{6}$$

For the normalization we take

$$\int d^3r\, P_i^* P_j = \pi r_o^2 \Lambda \tag{7}$$

where in the three dimensional spatial integral above, the z integral is taken only over a length L. Let us further take P_1 as being given by Eq.(4). If we assume that in the decomposition of the electric field, α_1 is nearly unity and all other α_i's are small, we can multiply Eq.(2) by P_1^*, integrate over space and find

$$-i(\omega - ckL/\Lambda) = (\pi r_o^2 \Lambda)^{-1} 2\pi \int_o^L dz \int d^2r\, J_x P_1^* \tag{7}$$

This then constitutes the dispersion relation. To complete the calculation, we must compute the right hand side, which is done in the next section. Notice that in the limit of zero current, the local wave number, kL/Λ is smaller than the wave number k characterizing the Floquet solution. This is so that when z changes by L, or l changes by Λ (which is longer than L), the phase change is the same. Also note that because the k value is much larger than $2\pi/L$, it is obviously not restricted to the first Brillouin zone (indeed there is no reason for the k to be in any particular zone). The index of the Brilloun zone is given approximately by $\omega\Lambda/2\pi c$.

3. Calculation of $\int P_1 * J_x$

To proceed, we calculate $\int P_1 * J_x$ for the configuration. We will calculate this only for the configuration of Fig.(1), and later will simply state the results for Fig.(2). In each periodicity length the electron beam the intersects the radiation twice, once going up, and once going down. In each vertical leg, the electric field is given by

$$\mathbf{E} = E_o \mathbf{i}_x \exp -(r/r_o)^2 \exp i((-1)^m ky - \omega t + \Phi_m) \tag{9}$$

where $(-1)^m$ accounts for the change in direction in the m^{th} vertical leg, and the Φ_m accounts for the phase change from one leg to another. Let us say that the distance between up and down leg is N. Then we can say

$$E = E_u \exp i(ky - \omega t) + E_d \exp i(-ky - \omega t + \Phi) \tag{10}$$

where

$$E_u = E_o \exp -(z/r_o)^2, \quad E_d = E_o \exp -((z-N)/r_o)^2 \tag{11}$$

In Eqs.(10 and 11), it is now understood that E is in the x direction, z, the distance along the magnetic field on which the beam propagates now replaces the transverse variable r.

Expressing the electric field on the two vertical legs in the form of Eq. (3 and 4), and Fourrier decomposing the periodic function P, we find

$$E(y,z) = \sum_n \sqrt{\pi} E_o (r_o/L) \exp[-(k+q_n)^2 r_o^2/4] \exp i(k+q_n)z$$
$$x\{\exp\ iLky/\Lambda + \exp\ i[\Phi - (k+q_n)P] \exp -iLky/\Lambda\} \exp i(kz - \omega t) \tag{12}$$

where $q_n = 2\pi n/L$. We now use this electric field in the linearized Vlasov Equation to calculate the perturbed distribution function and from it, the perturbed current. The calculation reported here closely parallels the analysis of Vomvoridis et al[11]. There the independent variables were the guiding center variables, related to the normal Cartesian variables by

$$p_x = p_\perp \cos(\Omega m z/p_z + \phi) \quad (a)$$
$$p_y = p_\perp \sin(\Omega m z/p_z + \phi) \quad (b) \qquad (13)$$
$$x = x_g + (p_\perp/m\Omega)\sin(\Omega m z/p_z + \phi) \quad (c)$$
$$y = y_g - (p_\perp/m\Omega)\cos(\Omega m z/p_z + \phi) \quad (d)$$

Then the linearized Vlasov Equation, in these variables becomes

$$(\partial/\partial z - i\gamma m\omega/p_z)f = G(z) \qquad (14)$$

where

$$G(z) = (\gamma meE(z)/\omega p_z)\{2\omega p_\perp \cos(\Omega m z/p_z + \phi)\partial f_o/\partial p_\perp{}^2\} \qquad (15)$$

where f_o is the unperturbed distribution function and γ is the relativistic factor and Ω is the cyclotron frequency. In Eq.(15) we have included only the velocity gradient terms, and neglected the terms arising from gradients in x_g and y_g. These typically give small corrections, and have been discussed in Ref.(10). The perturbed distribution function f is then given by

$$f = \exp[i\gamma m\omega z/p_z] \int^z dz' \exp[-i\gamma m\omega z'/p_z] G(z') \qquad (16)$$

From the perturbed distribution function, we calculate the perturbed current

$$J_x = -e\int d^3p \, (p_x/m\gamma) f \qquad (17)$$

The quantity to calculate then is the integral of $P_1 * J_x$ over the transverse cross section and over a periodicity distance L. Without going into the details of the calculation (it is quite analogous to that in Ref.(10)), we find that

$$\int P_1 * J_x = -A\int d^2r_g d^3p \sum_{n,s} [\exp -(k+q_n)^2 r_o{}^2/2]\{2J'_s{}^2(Lkp_\perp/\gamma m\Omega\Lambda)$$

$$x 2\omega p_\perp{}^2/p_z\}\partial f_o/\partial p_\perp{}^2/i[k+q_n + (s\Omega m - \gamma m\omega)/p_z] \qquad (18)$$

where $A = \pi\gamma e^2 E_o r_o{}^2/\omega L^2$. Now for the distribution function, take

$$f_o = I \, \{g(r_g)m\gamma/2\pi e p_z\} \, \delta(p_\perp{}^2 - p_{\perp o}{}^2) \, \delta(p_z - p_{zo}) \qquad (19)$$

where I is the beam current and $g(r_g)$ is the distribution of guiding centers, normalized so that $\int d^2r_g g(r_g)=1$. Notice that the distribution function is assumed to be unperturbed by its interaction with the radiation upstream from the periodicity length considered. This is examined more fully in the appendix where it is shown that this interaction (a klystron type interaction) has a negligible effect, at least in the linear regime.

Consistent with our assumptions of neglecting the various derivatives with respect to r_g in the derivation of J_x, we assume that the variation of $g(r_g)$ is small over distances compared to k^{-1}. To do the integral on the right hand side of Eq.(18), we perform a partial integration over $p_\perp^2$, and keep only those terms which arise from a differential of the resonant denominator. These terms are the ones which have that denominator raised to the second power, and are the largest terms if the wave frequency is nearly equal to the cyclotron harmonic. To continue, we approximate the effect of thermal spread in the beam. For the distribution function, let us assume that the beam energy (characterized by γ or the magnitude of the momentum p) is the same for all particles, but there is a distribution of pitch angle α ($p_z/p = \cos\alpha$). This pitch angle spread, assumed to be small, is characterized by $\delta\alpha$. We consider the effect of pitch angle spread only in the resonant denominator. For small $\delta\alpha$ this is the only place where its effect can be significant. The integral over p_z can be done analytically if the distribution of pitch angle is approximated by a Lorentzian

$$f(\alpha) = \{\pi[(\alpha-\alpha_o)^2 + (\delta\alpha)^2]\}^{-1} \qquad (20)$$

In this case the distribution of p_z is also Lorentzian centered at p_{zo} and having thermal spread $p_{\perp o}\delta\alpha$. While we cannot use the Lorentzian to accurately calculate the effect of a pitch angle spread, it should give a reasonable extimate of when the spread has a significant impact on the growth rate.

If we assume that the cyclotron harmonics are all decoupled, then the dispersion relation can be written in the form

$$-\omega\Lambda/cL + k = \sum_n H_s [1 - ip_\perp \delta\alpha/p_z]^{-2} \exp -0.5[(q_n + k)r_o]^2$$

$$x[k + q_n + m(s\Omega - \gamma\omega)/(p_z - ip_\perp \delta\alpha)]^{-2} \qquad (21)$$

where to simplify the notation, in Eq. (21) we have deleted the zero subscripts on the momentum variables. Here,

$$H_s = 16\gamma e\omega p_\perp^2 I J'^2_s (Lkp_\perp/\gamma m\Omega\Lambda) / (p_z^3 c^3 L^2) \qquad (22)$$

This then summarizes our result for the configuration of Fig 1. For that in Fig 2, an analogous calculation gives the result

$$-\omega\Lambda/cL + k = \sum_n [H_s'/\sin^2\beta] [1 - ip_\perp \delta\alpha/p_z]^{-2} \qquad (23)$$

$$x \exp -0.5[(q_n + k)r_o/\sin^2\beta]^2 x[k + \omega\cos\beta/c + q_n + m(s\Omega - \gamma\omega)/(p_z - ip_\perp \delta\alpha)]^{-2}$$

where β is the angle of the ray path to the horizontal in Fig 2 and

$$H_s' = 16\gamma e\omega p_\perp^2 I J'^2_s (Lkp_\perp \sin\beta/\gamma m\Omega\Lambda) / (p_z^3 c^3 L^2) \qquad (24)$$

The summation in $\int P_1^* J_x$ is a summation over various spatial harmonics of the mode structure, each spatial harmonic having a different resonant denominator. As long as the spatial growth rate Imk is much less than $2\pi/L$, the spatial harmonics can be considered one at a time, the spatial harmonic with $k=-q_n$ being the dominant one. Ultimately, these spatial harmonics become small due to the cutoff of the Gaussian $\exp -(k+q_n)^2 r_o^2/2$. Hence the amplifier can typically operate at some small number of spatial harmonics before the interaction strength becomes negligibly small. Thus the fact that the system is periodic with periodicity length L is extremely important in that it breaks the eigenfunction into this summation over space harmonics. These space harmonics are sufficiently separated in wave number that the interaction effectively proceeds with only one of them at a time. This greatly increases the strength of the interaction in the same way that a monoenergetic beam interacts more strongly with a wave than does a thermal distribution. It is not difficult to show that for a single resonator, the summation over k becomes an integral, and the conventional expression (with no resonant denominator) is obtained.

In each of these, the assumption is that the radiation mode and beam each propagate from left to right. This is the usual forward wave amplifier situation. For the case of the radiation mode propagating from right to left, the backward wave case, the dispersion relations are the same except that the sign of the k term on the left hand side becomes negative. These simple dispersion relations then summarize the basic theoretical results obtained up to now.

4. Instability condition

In a traveling wave amplifier, the forward wave interaction cannot be absolutely unstable, but the backward wave can be We calculate the stability threshold, paralleling an earlier calculation[12]. We only consider the worst case of zero thermal spread, and only the fundamental cyclotron frequency. Then the backward wave dispersion relations, taking only a single spatial harmonic, derived in the last section all had the form

$$k(k-\Delta)^2 = -K_0^3 \qquad (25)$$

where Δ and K_0 are both real. For the beam energies we consider, K_0 decreases as a function of cyclotron harmonic number. As we will see, the stable length of an amplifier is expressed as coefficient to be derived, divided by K_0. Therefore, all cyclotron harmonics above n will be stabilized if harmonic n is itself stabilized. This important result for the quasi-optical gyro TWA follows directly from the very simple nature of the spectrum, especially the absence of cutoff modes. In other gyro TWA experiments, important competing modes have turned out to be cutoff modes at higher harmonics.

Consider the amplification as arising from the coupling of a beam mode with amplitude W_1 and a radiation mode with amplitude W_2. The system is described by the two equations

$$(k-\Delta)^2 W_1 = -K_0^2 W_2 \qquad \text{(a)}$$

$$kW_2 = K_0 W_1 \qquad \text{(b)} \qquad (26)$$

This is cubic system, so there are three generally complex roots denoted k_1, k_2 and k_3. The coefficients of the three exponentials are denoted ξ_1, ξ_2, and ξ_3. Then consider a system of length Ψ. The beam mode convects from left to right, entering at z=0. The radiation mode convects from right to left, entering the system at $z=\Psi$. The condition for instability is then that if no beam mode enters at 0, and no radiation mode enters at Ψ, there will be a radiation mode of amplitude W_{20} exiting the system at z=0. Since the beam mode is described by a second order equation, the condition for no beam mode at the entrance means that both W_1 and its derivative vanish

at z=0. Regarding the exponential as solutions for W_1, we find that the equations for the three mode amplitudes are

$$0 = \xi_1 + \xi_2 + \xi_3 \qquad \text{(a)}$$

$$0 = ik_1\xi_1 + ik_2\xi_2 + ik_3\xi_3 \qquad \text{(b)} \qquad (27)$$

$$W_{20} = (K_o/k_1)\xi_1 + (K_o/k_2)\xi_2 + (K_o/k_3)\xi_3 \qquad \text{(c)}$$

The condition for instability is then that the amplitude of W_2 at $z=\Psi$ vanishes, or

$$(\xi_1/k_1)\text{expik}_1\Psi + (\xi_2/k_2)\text{expik}_2\Psi + (\xi_3/k_3)\text{expik}_3\Psi = 0 \qquad (28)$$

Solving for the coefficients, the instability condition becomes

$$[(k_3-k_2)/k_1]\text{expik}_1\Psi + [(k_1-k_3)/k_2]\text{expik}_2\Psi + [(k_2-k_1)/k_3]\text{expik}_3\Psi = 0 \qquad (29)$$

If Ψ is very small compared to the reciprocal of the k's, which in turn scale with K_o, clearly there is no solution to Eq.(29) and the system is stable. As Ψ increases, the oscillatory nature of the exponentials will allow the summation to equal zero. At some length Ψ_o, there will first be a value of $\Delta=\Delta_o$ for which the summation vanishes. At this point there can be a solution of a non zero outgoing radiation mode with no inputs of either radiation or beam mode. The Δ_o then determines the frequency of the instability, and the Ψ_o determines the maximum length (or beam current) of the stable system.

A numerical solution of the dispersion relation gives the result

$$\Delta_o = -3.003/K_o \qquad \text{(a)}$$

$$\Psi_o = 7.68/K_o \qquad \text{(b)} \qquad (30)$$

5. Results and Discussion

Let us begin by considering a possible configuration for both the quasi-optical and corrugated waveguide configuration. For normal incidence, if the mirror has radius of curvature R_m, and half the separation between the mirrors is L_y, then the radiation spot size at the center is given by[13]

$$r_o = [\lambda L_y(R_m/L_y - 1)^{1/2}/\pi]^{1/2} \tag{31}$$

where λ is the radiation wavelength. The spot size at the mirror then turns out to be

$$r_{om} = [\lambda L_y(R_m/L_y - 1)^{-1/2}/\pi]^{1/2} \tag{32}$$

If we take a spot size r_o of 0.5cm, a wavelength of 0.3 cm, and L_y of 3 cm, we find that the mirror radius R_m is about 5 cm and the spot size at the mirror is about .62 cm. To reduce diffraction loss, the mirror size should be a radius of about 1.5 cm. Since the mirror is tilted at 45°, the total half length of the mirror in the vertical direction is about 2 cm, so the vertical ray path is about 10 cm. Hence a magnet bore of roughly 4 inches should be sufficient to hold the tube. If the facing mirror edges are two centimeter apart, the horizontal length of the ray path is L=10 cm, and the total ray path within the periodicity cell is Λ = 22 cm.

The corrugated waveguide propagates TEM modes with E_x proportional to $J_o(2.4r/a)$, with very low loss. If this mode is decomposed into a summation of Gaussian modes with r_o = 0.64a, then about 98% of the poower is in the fundamental Gaussian mode[14]. Thus the Gaussian mode is an excellent approximation to the field in the corrugated waveguide as well. For this case an important consideration is the loss on transiting the gap and on reflection at the mitre bends. According to Doane and Moeller[15,16] the loss on transiting the gap is given by

$$\begin{aligned} &\text{Gap Loss (db)} = 1.7\ [Q\lambda/2a^2]^{3/2} \\ &\text{Mitre Bend Loss (db)} = 0.85\ [\lambda/a]^{3/2} \end{aligned} \tag{33}$$

where a is the waveguide radius and Q is the gap space. For our case of λ =0.3 cm, a waveguide radius of 1.5 cm and a gap length of also 1.5 cm, we find that there is a 1.2% loss at each gap and a 1.7% loss at each mitre bend. Since there are 2 gaps and 4 mitre bends in each periodicity length L, there is about a 9% loss in the periodicity cell. This loss is only loss from the TEM mode; much of the lost power is still bouncing around the waveguide. If the wave amplifies strongly from one periodicity cell to the next, the output radiation should be about 90% in the desired mode.

Now let us evaluate the growth and bandwidth from the dispersion relations calculated in Section 3. We consider only the case where the space harmonics decouple from one another, so that the beam interacts with only one of them. The use of a single spatial harmonic itself puts a limit on the bandwidth which can be accurately calculated. Since $k \approx \omega\Lambda/cL$, and a change in k of $2\pi/L$ brings us to the next spatial harmonic, the maximum accurate bandwidth we can calculate with a single spatial harmonic is about 1.5 GHz for the parameters specified.1.5 GHz.

If we define

$$K = k - \omega\Lambda/cL$$

and assume, strictly for simplicity sake that the cyclotron frequency corresponds exactly to cLq_n/Λ, and define $\omega = s\Omega/\gamma + \delta\omega$, where s is the cyclotron harmonic, we find that the dispersion relation for a cold beam is

$$K[K-\Delta]^2 = K_o^3 \qquad (34)$$

If both K and Δ are scaled with K_o, then K/K_o is a function of only the single parameter Δ/K_o. A numerical solution for the fastest growing root is shown in Fig.(8). The minimum growth length turns out to be about $1.2/K_o$.

Let us consider an interaction at the cyclotron frequency for a configuration like that shown in Fig.(1). In this case, we find that

$$K_o^3 = [4\gamma I e p_\perp^2 \omega]/[p_z^3 c^3 L^2] \qquad (a)$$

(35)

$$\Delta = [\Lambda/cL - \gamma m/(p_z - i p_\perp \delta\alpha)]\delta\omega \qquad (b)$$

where we have actually included the effect of the thermal spread in the resonant denominator. Let us consider a particular beam for this configuration. Take an energy of 100 kV, a value of tan α of 1.5 and no thermal spread. This is a fairly high value for an amplifier configuration. However our hope is that this configuration will be much more stable than a waveguide configuration, for which such a high value of $p_\perp/p_z$ would almost surely be unstable. Then if $\omega = 6 \times 10^{11}$ s^{-1}, we find that

$$K_o^3\ (cm^{-3}) = 3.2 \times 10^{-2}\ [I(Amps)/L^2(cm^2)] \qquad (36)$$

Thus if we consider a beam of ten amps and L=10 cm, the minimum growth length is about 8 cm, and maximum stable length is about 60 cm. One real advantage of the configuration of Fig.(1) is that it is not very sensitive to beam thermal spread. As is apparent from Eq.(35b), the condition for neglect of thermal spread at the band center ($\delta\omega = 0$) is

$$p_z >> p_\perp \delta\alpha \qquad (36)$$

a condition not very difficult to satisfy for typical gyrotron beams. As $\delta\omega$ increases however, the effect of thermal spread becomes more pronounced because of its contribution in the resonant denominator. As a function of $\delta\omega$ the condition for the neglect of thermal spread is

$$\delta\alpha\ \delta\omega/v_z << K_o \qquad (37)$$

For the beam parameters we have chosen, and $\delta\omega$ chosen to be 2π times 1.5 GHz, we see that the maximum allowed angular spread is about 10^{-1} radians.

Let us now calculate the bandwidth, for the cold beam, in the linear regime. Imagine that the input power is 100 W and the output power is 10^5 W, so the power gain is a thousand. This is about 3.5 e folds in amplitude. At the band edge, the power is down by a factor of 2, or the amplitude by factor of 1.4, (ie exp0.3). From

the graph in Fig.(8), this gives a spread in Δ/K_0 of about 2. For the parameters chosen this means a bandwidth of about 1.5 GHz, the maximum accurate bandwidth. Thus a more accurate calculation of the bandwidth must involve the calculation of the simultaneous interaction of several spatial harmonics and thermal spread.

At the cyclotron harmonic, for the same system except now a beam energy of 150 kV, we find that K_0^3 is smaller by about a factor of 0.28, so the minimum growth length now turns out to be about 12 cm. The total length must still be below that determined for the cyclotron frequency instability however, or else severs or directional couplers would have to be used.

Finally, let us consider the configuration of Fig.(2). Here, interaction strengths and bandwidths are somewhat larger, and required magnetic fields are somewhat lower, because of the Doppler shift provided by the beam's velocity parallel to the direction of propagation. However this seems to be counterbalanced by the fact that the beam requirements are much more difficult to achieve. From Eq.(23), the requirements on beam thermal spread are given by

$$Kp_z >> p_\perp \delta\alpha(\omega/c)\cos\beta \qquad (38)$$

This is a much more difficult condition to satisfy. For the beam parameters we have been taking, this would mean an α spread of about a percent or less.

Appendix The Effect of Prebunching in the Linear Regime

Here, we consider the effect on $P_1 * J_x$ from the the upstream periodicity elements. That is in Sec. 3, when calculating $P_1 * J_x$, we assumed that the input distribution function was a delta function in $p_\perp$, p_z, and had uniform distribution in azimuthal angle ϕ. However actually, the beam, by the time it enters the periodicity unit in question, has passed through all of the periodicity units upstream. Thus the distribution function is actually not a delta function, but must also reflect the interaction with the upstream cavities. Here we consider the effect of this interaction in the linear regime. We show that the effect is very small compared to those retained in Sec.3.

We only consider the effect from the nearest upstream periodicity unit, and also consider only the effect of prebunching from that part of the radiation going in the same direction in y in each unit. As we will see, there are phase averages, which nearly vanish, involved in the integral of $P_1 * J_x$ calculated on the radiation going up in y, resulting from the prebunching of the electron beam, in the nearest upstream periodicity unit, from the radiation going down in y.

One can integrate the linearized equation for $p_\perp$ through the upstream radiation field and find that the wave going in the positive direction in y gives the the i^{th} electron of the beam a change in $p_\perp$ given by

$$\Delta p_{\perp i} = [\sqrt{\pi} e E_o r_o / 2 m v_z] \cos(\omega y_i / c - \omega t_i + \phi_i) \exp-[\Omega/\gamma - \omega]^2 r_o^2 / (2 v_z)^2 \quad (A1)$$

where y_i is the guiding center position of the entering electron, t_i is the entrance time, and ϕ_i is the entrance gyro phase.

The change in $\Delta p_{\perp i}$ gives a change to the γ of each electron, which in turn gives a change to its orbital frequency between the n-1 and n periodicity units. When it enters the next periodicity unit, the phase angle of the i^{th} electron is

$$\phi = \phi_i + \Omega L / \gamma v_z - \Omega L p_\perp \Delta p_{\perp i} / 2 \gamma^3 v_z m^2 c^2 \quad (A2)$$

Then, in the integral over t and ϕ integral for $P_1{*}J_x$, we transform these variables to t' and ϕ', and find that the linear expresion is given by

$$\int d^3r d^3p dt' \; P_1{*}J_x = \int d^3r d^3p dt' W \cos(ky+\phi_i-\omega t_i)\sin(\phi_i+\Omega z/\gamma v_z)$$

$$x\cos[ky-\omega(t_i+z/v_z) +\zeta] \; \exp-[(z+L)/r_o]^2 \qquad (A3)$$

where ζ is the phase shift in going across the periodicity unit and

$$W = \sqrt{\pi}[\Omega L e^2 E r_o p_\perp^2 f_0(p_\perp^2,p_z,\phi_i)/4m^3 v_z^2 \gamma^3] \qquad (A4)$$

$$x \; \exp-[(\Omega/\gamma - \omega]^2(r_o/2v_z)^2$$

Here, f_o is assumed to be distributed uniformly in ϕ_i. The trigonometric integral in Eq.(A4) breaks up into several terms which integrate to zero over phase. The one that does not is

$$\int d^3r d^3p dt' \cos^2(ky+\phi_i-\omega t_i) \; \sin\zeta \; \sin[(\Omega/\gamma-\omega)z/v_z]$$

Note that had the downward traveling wave provided the prebunching and the upward wave the extraction, the first factor above would have been, $\cos(ky+\phi_i-\omega t_i)\cos(-ky+\phi_i-\omega t_i)$, which would also integrate to zero over phase. Doing the phase integrals Eq.(A3), we find that

$$\int d^3r d^3p dt' \; P_1{*}J_x = W \;\; \sin\zeta \; \sin[(\Omega/\gamma-\omega)L/v_z] \qquad (A5)$$

$$x \; \exp-2[(\Omega/\gamma - \omega]^2(r_o/2v_z)^2$$

Thus in this contribution to the energy input, there is no resonant denominator rasied any power. Hence this term is but a small correction to those calculated in Sec.(3) which typically had denominators like $[(\Omega/\gamma - \omega]^{-2}$.

References:

1. B. Lax, Private communication, October, 1994

2. A. Ganguly, J. Choi and C. Armstrong, IEEE Trans Electron Devices, February, 1995.

3. R. Fischer, A. Fliflet, W. Manheimer, B. Levush, T. Antonsen, and V. Granatstein, Phys. Rev. Let. 72, 2395, (1994)

4. R. Fischer, A. Fliflet, W. Manheimer, Phys. Fluids, B5, 2682, (1993)

5. R. Temkin, private communication, January, 1995

6. A. Fliflet, T. Hargreaves, W. Manheimer, R. Fischer, M. Barsanti, B. Levush and T. Antonsen, Phys. Fluids, B2, 1046, (1990)

7. A. Fliflet, T. Hargreaves, R. Fischer, W. Manheimer, and P. Sprangle, J. Fusion Energy, 9, 31, (1990)

8. W. D. Fitzgerald, Lincoln Laboratory Journal, Vol 5, No.5 (1992)

9. B. Lax, SPIE Proc. Vol. 2211, p4, (1994)

10. R. Collin, Foundations of Microwave Engineering, p299, McGraw Hill, 1966

11. J. Vomvoridis, P. Sprangle, and W. Manheimer, In Millimeter and Infrared Waves, Vol 7, p 487, (1983), K. Button ed.

12. A. Ganguly, G. Park, and C. Armstrong, Phys. Fluids, B5, 1639, (1993)

13. A. Yariv, Optical Electronics, Chap. 4, Holt, Rinehart and winston, New York, 1985

14. J. Leseuf, Millimeter Wave Optics, Devices and Systems, p55, Adam Hilger, Bristol, (1990)

15. J. Doane, Millimeter and Infrared Waves, Vol 13, p 123, (1985), K. Button, ed.

16. J. Doane and C. Moeller, GA Report GA-A21884

Acknowledgements

The author would like to thank Achintya Ganguly for a number of very helpful discussions. He also thanks, Benjamin Lax, John Braud and Jeffery McCarg of Lincoln Laboratory and John Doane of General Atomics for a number of useful dicsussions. This work was supported by ONR.

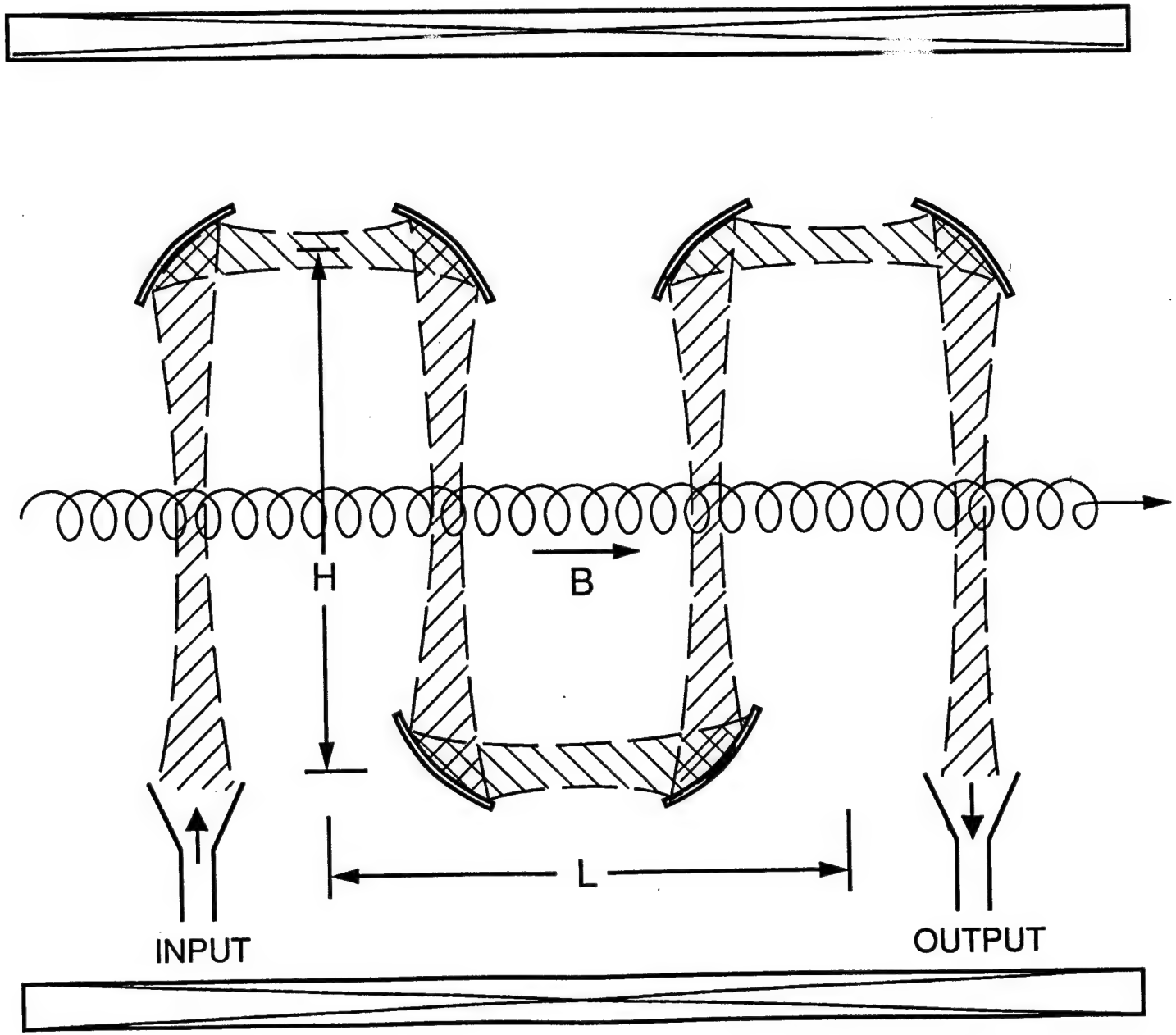

1. Schematic of the normal incidence quasi-optical gyro TWA.

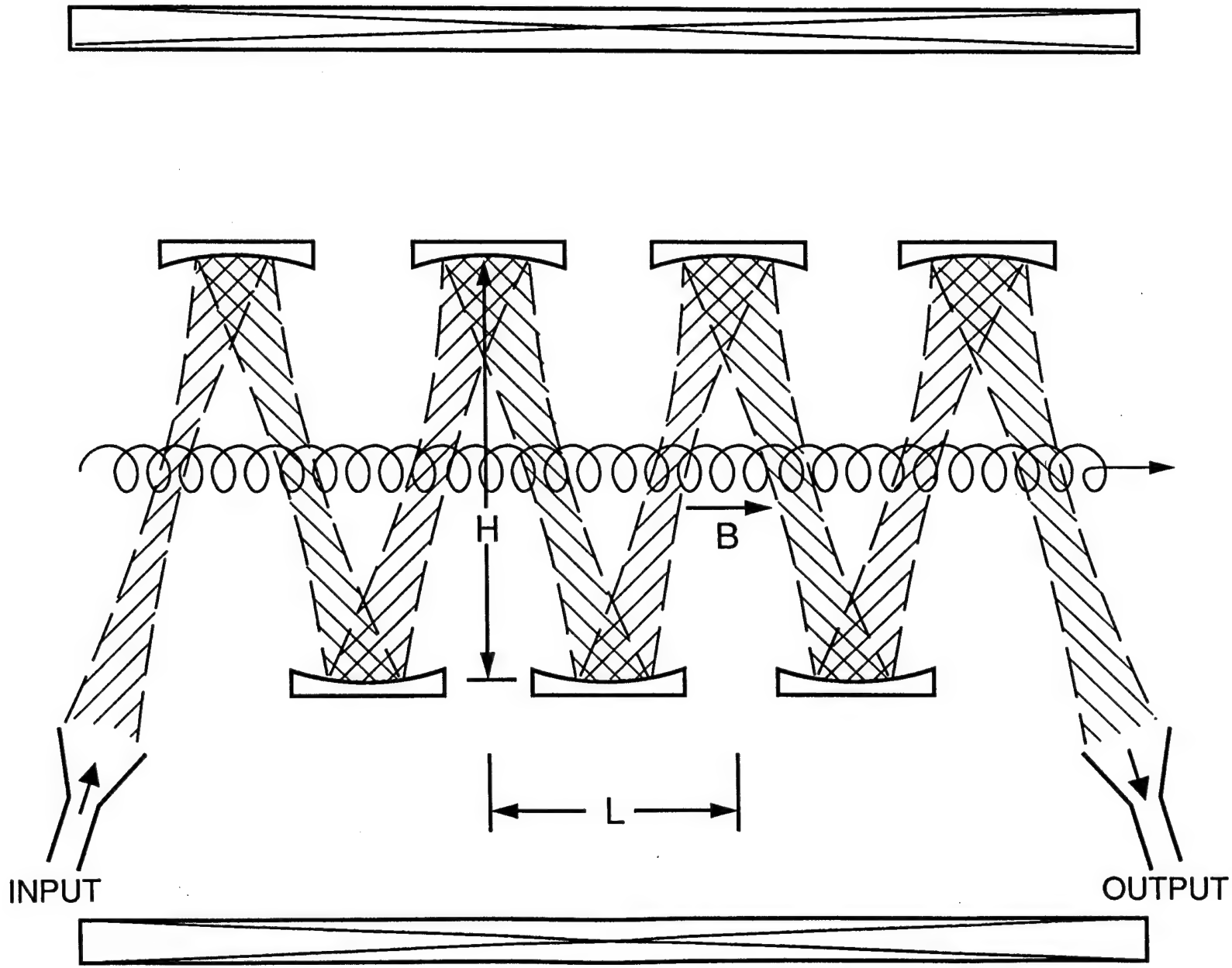

2. Schematic of the oblique incidence quasi-optical gyro TWA.

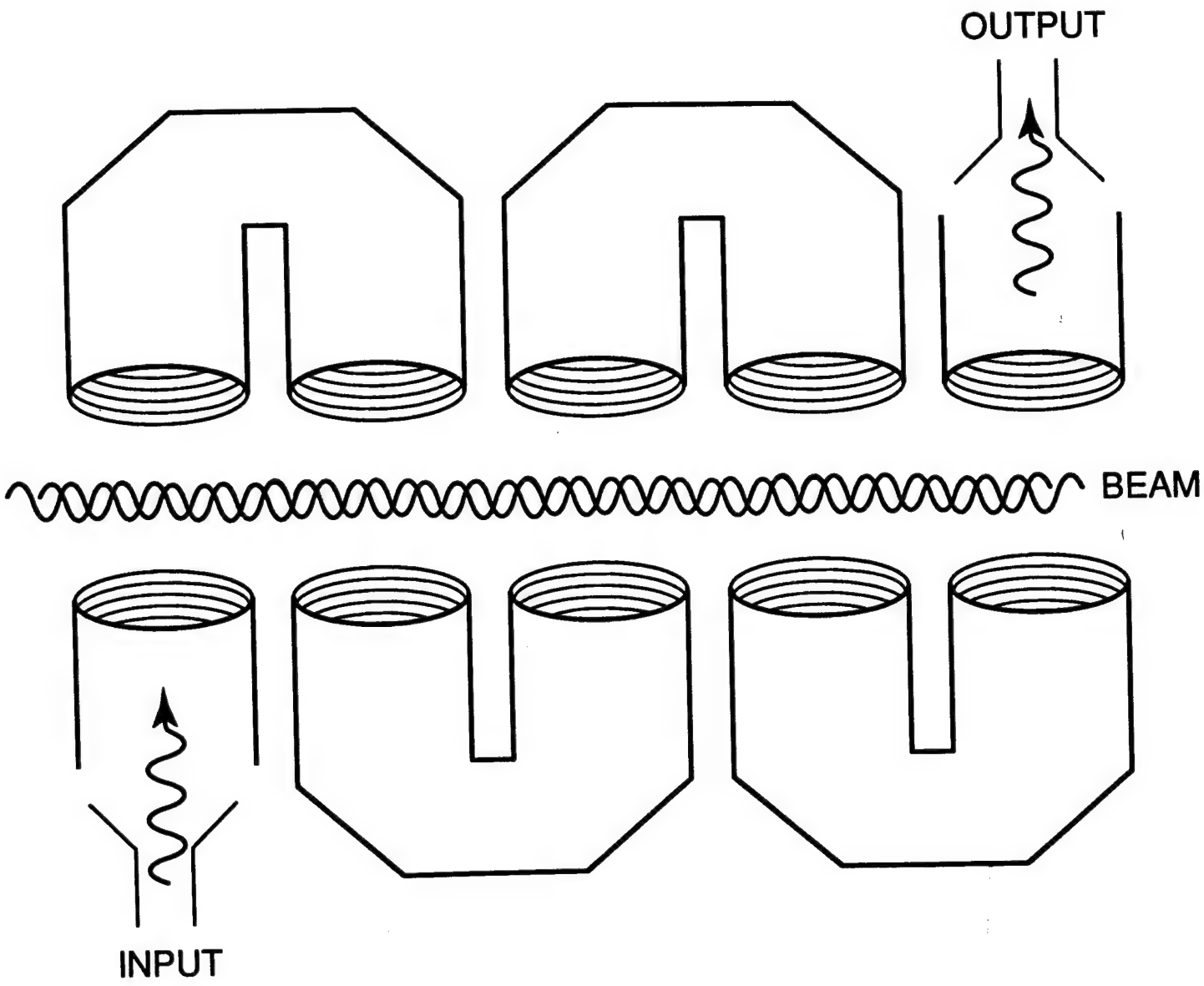

3. Schematic of the Gyro TWA in a corrugated waveguide.

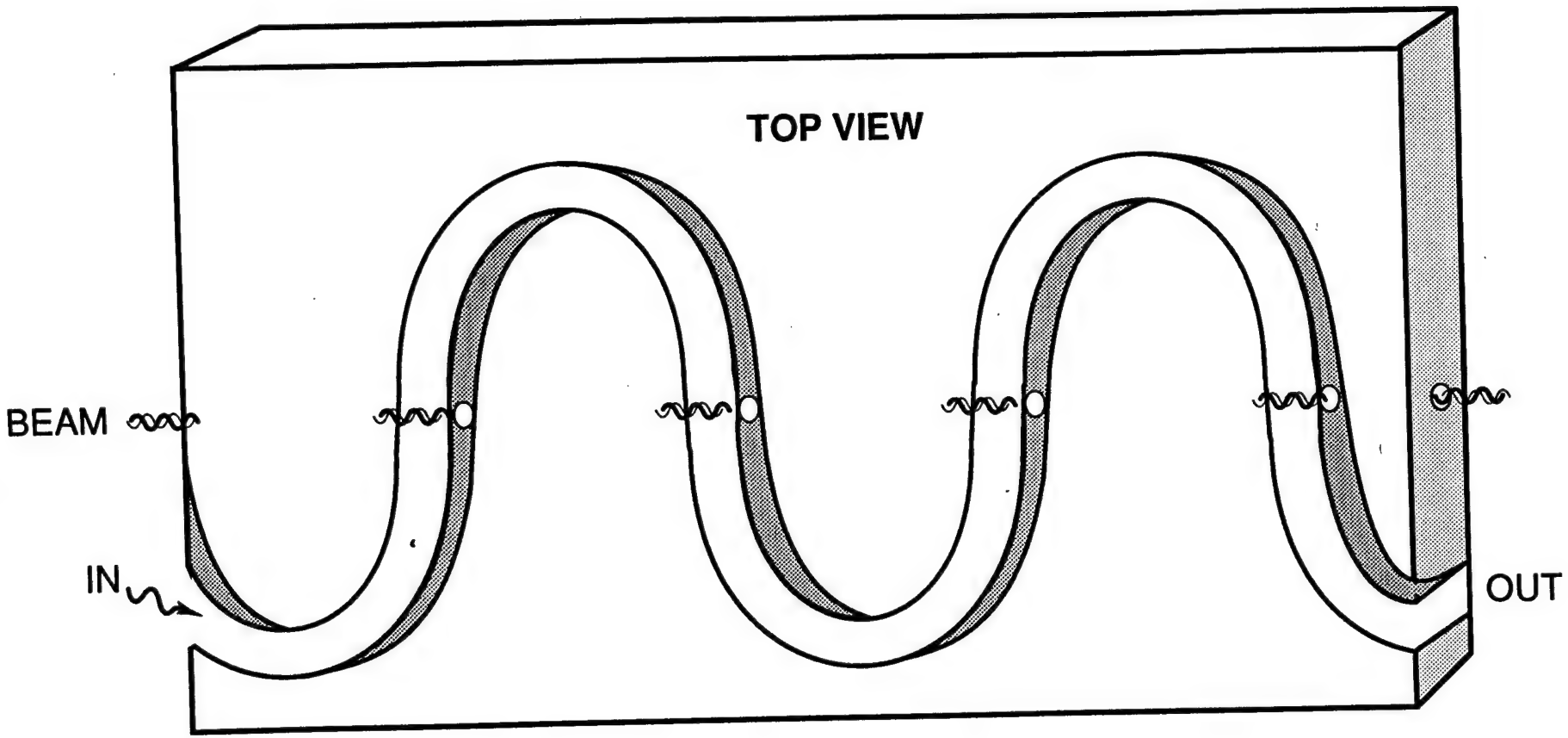

4. Schematic of the Folded waveguide TWA.

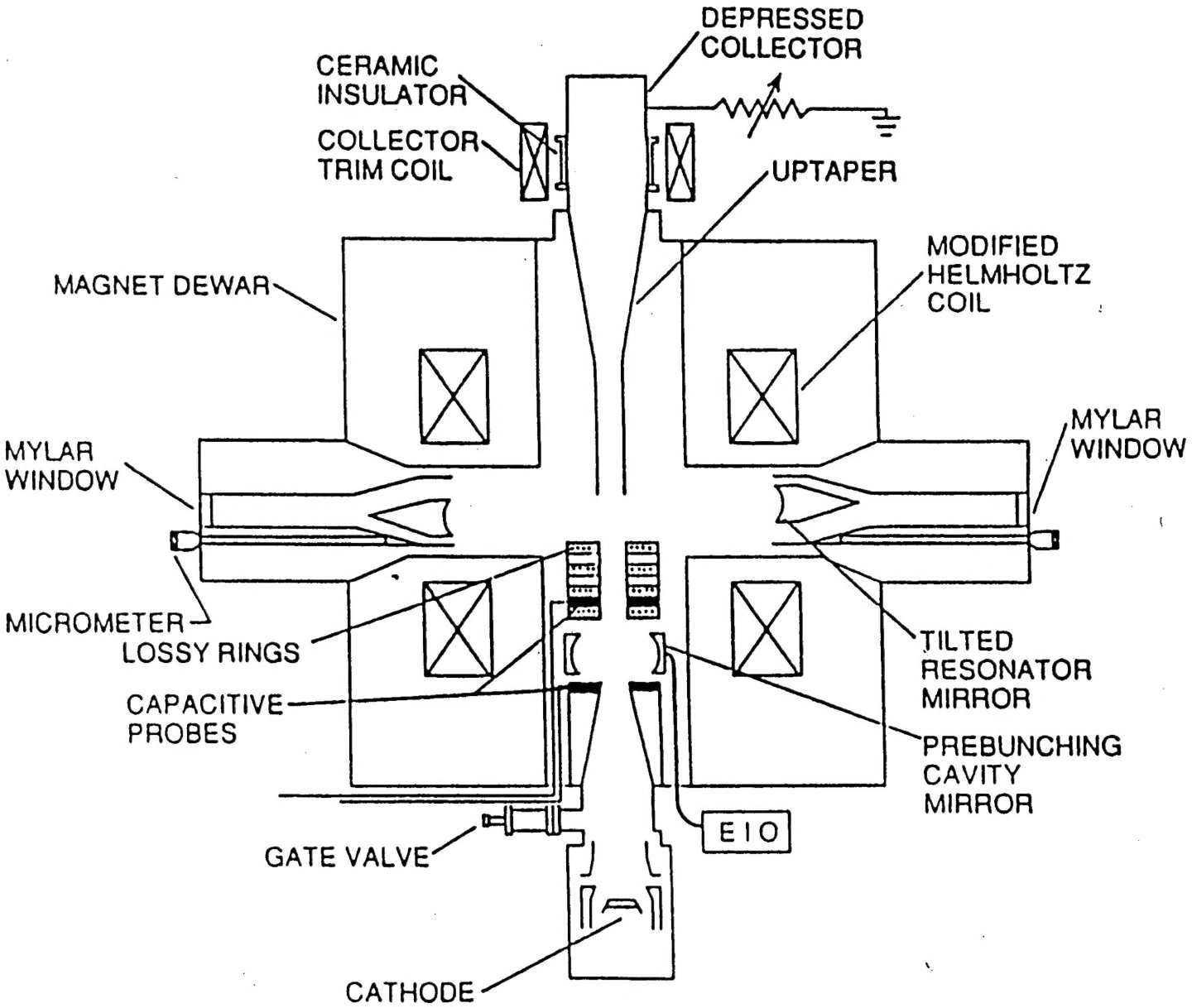

5. Schematic of the quasi-optical gyrotron and gyro klystron.

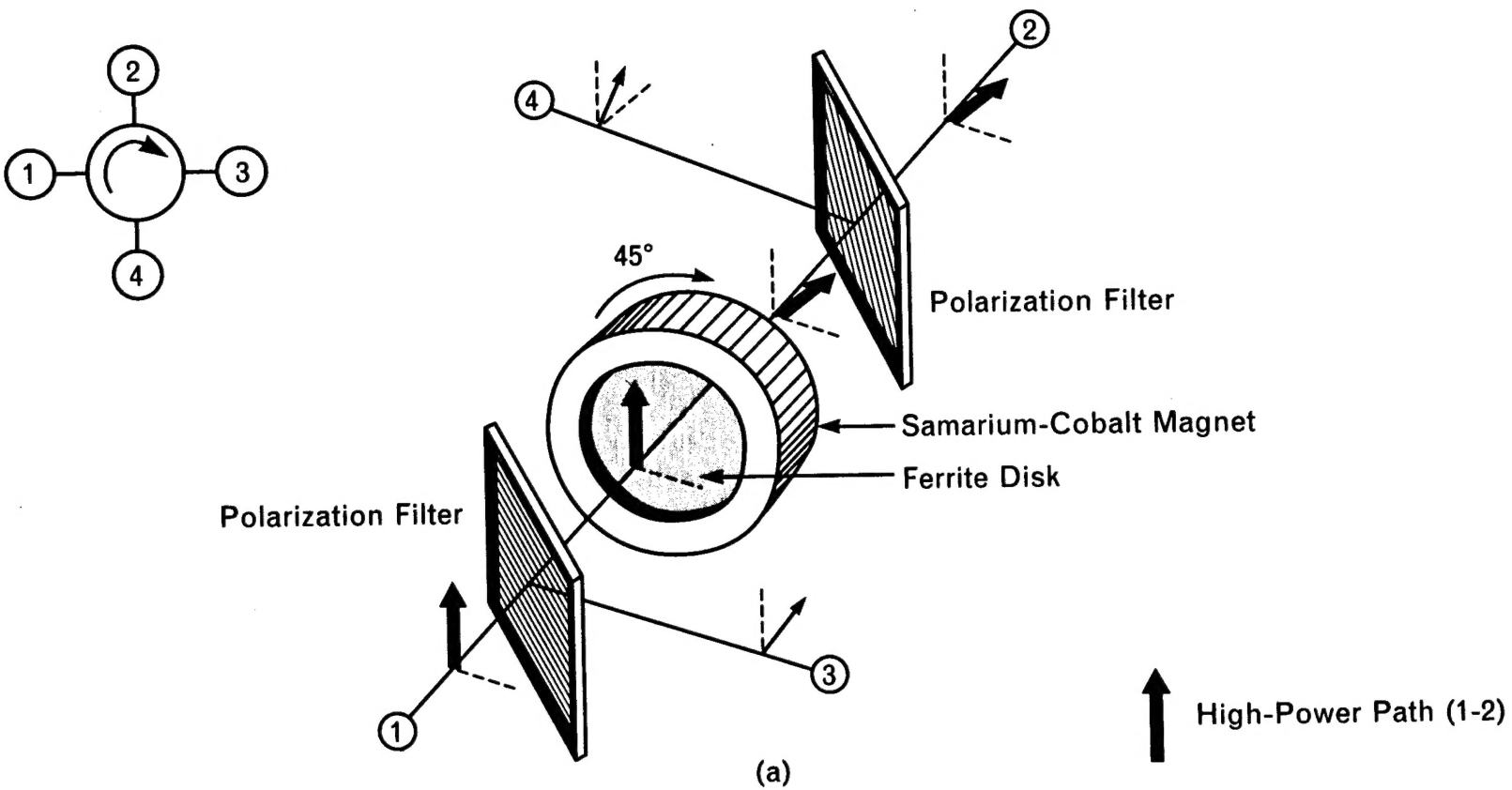

6. Schematic of the Lincoln Laboratory clam shell reflector.

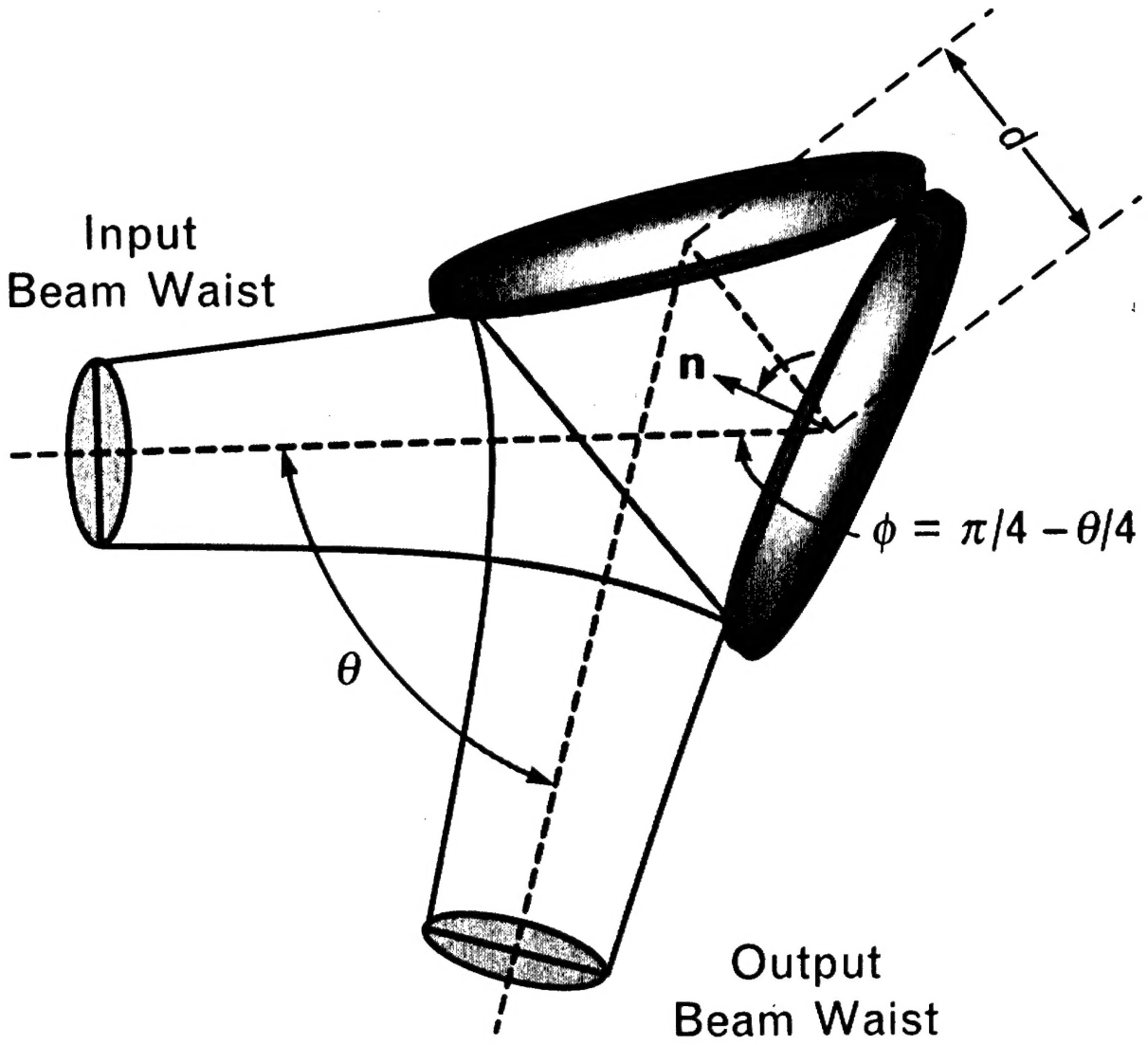

7. Schematic of the Lincoln Laboratory quasi-optical circulator.

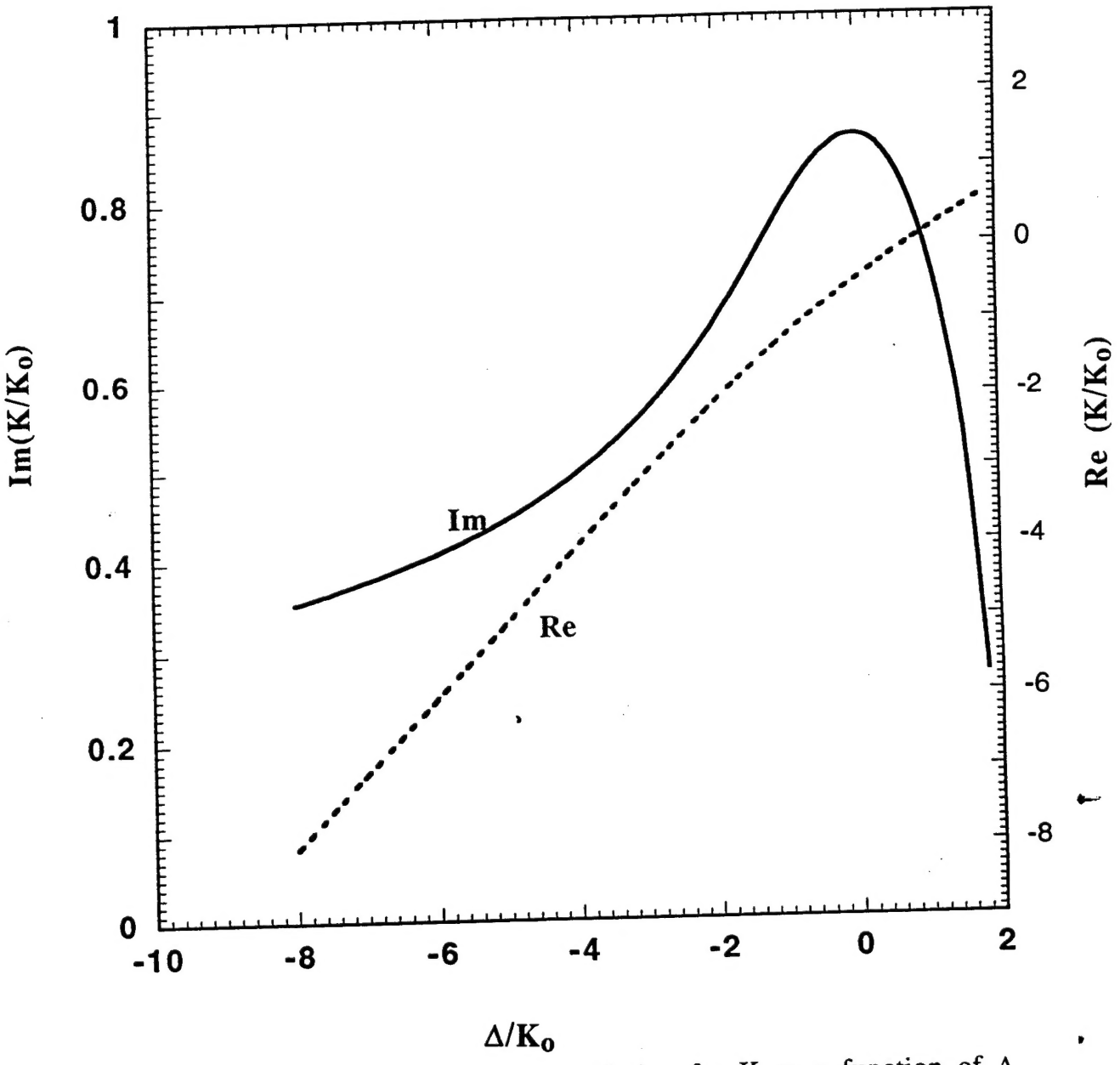

8. Solution of the dispersion relation for K as a function of Δ.